



# High-numerical-aperture and long-working-distance objective for single-atom experiments

Cite as: Rev. Sci. Instrum. **91**, 043104 (2020); <https://doi.org/10.1063/5.0001637>

Submitted: 19 January 2020 . Accepted: 17 March 2020 . Published Online: 10 April 2020

Shaokang Li, Gang Li , Wei Wu , Qing Fan, Yali Tian, Pengfei Yang, Pengfei Zhang , and Tiancai Zhang



View Online



Export Citation



CrossMark

Lock-in Amplifiers  
up to 600 MHz



Watch



# High-numerical-aperture and long-working-distance objective for single-atom experiments

Cite as: Rev. Sci. Instrum. 91, 043104 (2020); doi: 10.1063/5.0001637  
Submitted: 19 January 2020 • Accepted: 17 March 2020 •  
Published Online: 10 April 2020



Shaokang Li,<sup>1,2</sup> Gang Li,<sup>1,2,a)</sup>  Wei Wu,<sup>1,2</sup>  Qing Fan,<sup>1,2</sup> Yali Tian,<sup>1,2</sup> Pengfei Yang,<sup>1,2</sup> Pengfei Zhang,<sup>1,2</sup>  and Tiancai Zhang<sup>1,2,b)</sup>

## AFFILIATIONS

<sup>1</sup>State Key Laboratory of Quantum Optics and Quantum Optics Devices, and Institute of Opto-Electronics, Shanxi University, Taiyuan 030006, China

<sup>2</sup>Collaborative Innovation Center of Extreme Optics, Shanxi University, Taiyuan 030006, China

<sup>a)</sup>Author to whom correspondence should be addressed: [gangli@sxu.edu.cn](mailto:gangli@sxu.edu.cn)

<sup>b)</sup>[tczhang@sxu.edu.cn](mailto:tczhang@sxu.edu.cn)

## ABSTRACT

We present a long-working-distance objective lens with numerical apertures  $NA = 0.4$  for single-atom experiments. The objective lens is assembled entirely by the commercial on-catalog  $\Phi 1''$  singlets. The objective can correct the spherical aberrations due to the standard flat vacuum glass windows with various thicknesses. The typical working distance is 18.2 mm at the design wavelength of 852 nm with a 5-mm thick silica window. In addition, the objective can also be optimized to work at the diffraction limit at a single wavelength in the entire visible and near infrared regions by slightly tuning the distance between the first two lenses. The diffraction limited field of view is 0.61 mm, and the spatial resolution is 1.3  $\mu\text{m}$  at the design wavelength. The performances are simulated by using the commercial ray-tracing software and confirmed by imaging the resolution chart and a 1.18  $\mu\text{m}$  pinhole. The objective can be used for trapping and manipulating single atoms of various species.

Published under license by AIP Publishing. <https://doi.org/10.1063/5.0001637>

## I. INTRODUCTION

As one of the most important tasks in the field of quantum research, quantum computing<sup>1</sup> has been explored for decades based on various physical systems. The optically trapped neutral single-atoms system, which has the advantages of long coherence time and good scalability, has been regarded as one of the most promising systems to achieve quantum computation.<sup>2–4</sup> Very recently, demonstration of high-fidelity quantum gates via Rydberg interaction accelerated research on the neutral atom-based quantum computation.<sup>5,6</sup> The foundation of neutral atom-based quantum computing is the resolvable single atom array.<sup>7–13</sup> The objective lens systems, which possess the diffraction limited condition within a large field of view (FOV), high numerical aperture (NA), and long working distance (WD), are used in many experiments<sup>12–17</sup> to form the micro-sized optical dipole trap array and load single atoms from magneto-optical trap (MOT). In addition, the same

objective lens is usually adopted to observe the trapped single atoms. In order to be compatible with specific atomic species and vacuum chambers, the objective lenses are always custom designed and manufactured. This made them costly and time-consuming to be obtained.

Many substituting designs, mostly using the on-catalog commercial spherical singlet, appeared in recent years. The first one is the “Alt objective,”<sup>14</sup> which uses three pieces of commercial singlets and one piece of custom-designed singlet to realize a diffraction limited objective with  $NA = 0.29$ . All the singlets have a size of  $\Phi 1''$  in this design so that the objective is compatible to the commonly used  $\Phi 1''$  optics in the experiment. Later, several designs with all commercial  $\Phi 2''$  singlets were reported, and the diffraction limited NA is between 0.175 and 0.44 upon different designs.<sup>18–20</sup> All these designs provide more options for the single-atom experiments.

In this paper, we provide an additional design of the objective lens with all  $\Phi 1''$  on-catalog commercial singlets from Thorlabs, Inc.

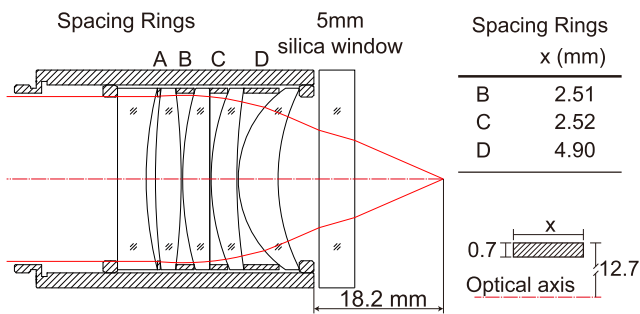


**FIG. 1.** Structure of the NA = 0.4 objective lens assembly. The five lenses from left to right are LC1120, LB1676, LA4380, LE1234, and LE5802 from Thorlabs. A is a standard 0.4-mm plastic spacer SM1S01 from Thorlabs. B, C, and D are three custom-made spacing rings.

The objective can correct the spherical aberrations due to the standard flat vacuum glass windows with various thicknesses. The typical NA and WD are NA = 0.4 and WD = 18.2 mm at a design wavelength of 852 nm with a standard 5 mm-thick silica vacuum window. The diffraction limited FOV is 610  $\mu\text{m}$ , and the resolution is 1.3  $\mu\text{m}$  at the design wavelength. The objective can be optimized to work at the diffraction limited condition for various thicknesses of vacuum window under a single wavelength in the entire visible and near infrared regions by slightly tuning one lens spacing. The performances are simulated by using the commercial ray-tracing software and confirmed by imaging the resolution chart and a 1.18  $\mu\text{m}$  pinhole.

## II. DESIGN

The structure of the lens assembly is shown in Fig. 1. Five commercial catalog singlets (LC1120, LB1676, LA4380, LE1234, and LE5802 from Thorlabs) are housed in the standard commercial  $\Phi 1''$  lens tube (SM1L10, Thorlabs) with three custom-made

**TABLE I.** NA = 0.4 objective prescription. The design wavelength is 852 nm. VW means vacuum window.

Surface	Curvature (mm)	Thickness (mm)	Material	Lens
1	$\infty$	4	NBK7	LC1120
2	51.5	1.3 (d)	Air	
3	102.4	3.6	NBK7	LB1676
4	-102.4	0.2	Air	
5	46	3.8	Silica	LA4380
6	$\infty$	0.2	Air	
7	32.1	3.6	NBK7	LE1234
8	82.2	0.2	Air	
9	15.5	5.6	CaF <sub>2</sub>	LE5802
10	28.0	5.0 (D)	Air	
11	$\infty$	5	Silica	VW
12	$\infty$	13.17	Vacuum	

spacing rings (B, C, and D) and a 0.4-mm plastic spacer (A: SM1S01, Thorlabs). The drawing and size of the rings are also shown in Fig. 1. Two retaining rings (SM1RR, Thorlabs) are used to fasten the assembly. The complete prescription of the objective designed for the 5 mm-thick silica vacuum flat window at 852 nm is given in Table I.

## III. PERFORMANCE

The performance of the objective is optimized and simulated by using the commercial ray-tracing software (Zemax). The comparison of the simulated modulation transfer function (MTF) for focal spots on axis and 300  $\mu\text{m}$  off axis to the diffraction limited MTF is shown in Fig. 2(a). The calculated Strehl ratio vs off-axis displacement is displayed in Fig. 2(b) as the solid red line. We can see that the MTF of our objective is almost overlapped with the ideal one and the Strehl ratio is 1 when the focal spot is on axis, which means that our objective lens has corrected the spherical error perfectly. The off-axis performance is little bit worse. The diffraction limited FOV is usually defined as the displacement from the axis where the Strehl ratio  $\geq 0.8$ .<sup>21</sup> From Fig. 2(b), we can see that the theoretical FOV for our objective is 0.61 mm.

To experimentally verify the performance of the objective, a USAF 1951 resolution target (55-622, Edmund Optics) and a 1.18  $\mu\text{m}$  pinhole (P1H, Thorlabs) are used to evaluate the objective by imaging them on a CCD camera (UC500M, CatchBest) with a  $f = 500$  mm achromatic lens (AC254-500-B, Thorlabs). A collimated 852-nm laser beam is used to illuminate the objects, and a 5 mm fused silica flat was adopted to imitate the vacuum window. The 500-mm achromatic lens is placed right after the objective, and the CCD camera is placed at the focal point of the achromatic lens.

The image of the resolution target is shown in Fig. 2(c), and the magnification of the imaging system can be determined as -17.68 from the image by considering the pixel size ( $2.2 \times 2.2 \mu\text{m}^2$ ) of the camera. We can see that the line pairs in element 4 of group 8 can be clearly resolved, and this means that a resolution about 1.4  $\mu\text{m}$  can be achieved. The result is consistent with the theoretical resolution  $0.61\lambda/\text{NA} = 1.3 \mu\text{m}$ . Next, by imaging the 1.18  $\mu\text{m}$  pinhole, the point spread function (PSF) is measured. Figures 2(d)-2(f) show the results with the pinhole placed -300  $\mu\text{m}$ , 0  $\mu\text{m}$ , and 300  $\mu\text{m}$  off the optical axis. The insets of each figure are the corresponding images of the pinhole. The measured intensity distribution along the x-axis and y-axis is shown as red open circles and blue open squares, respectively. The black solid curves are the theoretical intensity distribution with an ideal lens system, and the curve is given by the convolution between a 1.18  $\mu\text{m}$  top-hat function and the ideal PSF. The theoretical curve is normalized to the maximum intensity, while all the experimental data are normalized as the overall power same to the theoretical one. Therefore, the maximum intensity on the experimental data represents the measured Strehl ratio,<sup>21</sup> and they are shown as  $S_x$  and  $S_y$  for the two directions in each figure. We can see that the average Strehl ratios for the three positions of the pinhole are no less than 0.8. The results confirm that the diffraction limited FOV of our objective lens is greater than 0.6 mm.

In fact, the third plano-concave silica lens (LA4380) can be replaced by the counterpart made from N-BK7 (LA1509). In this

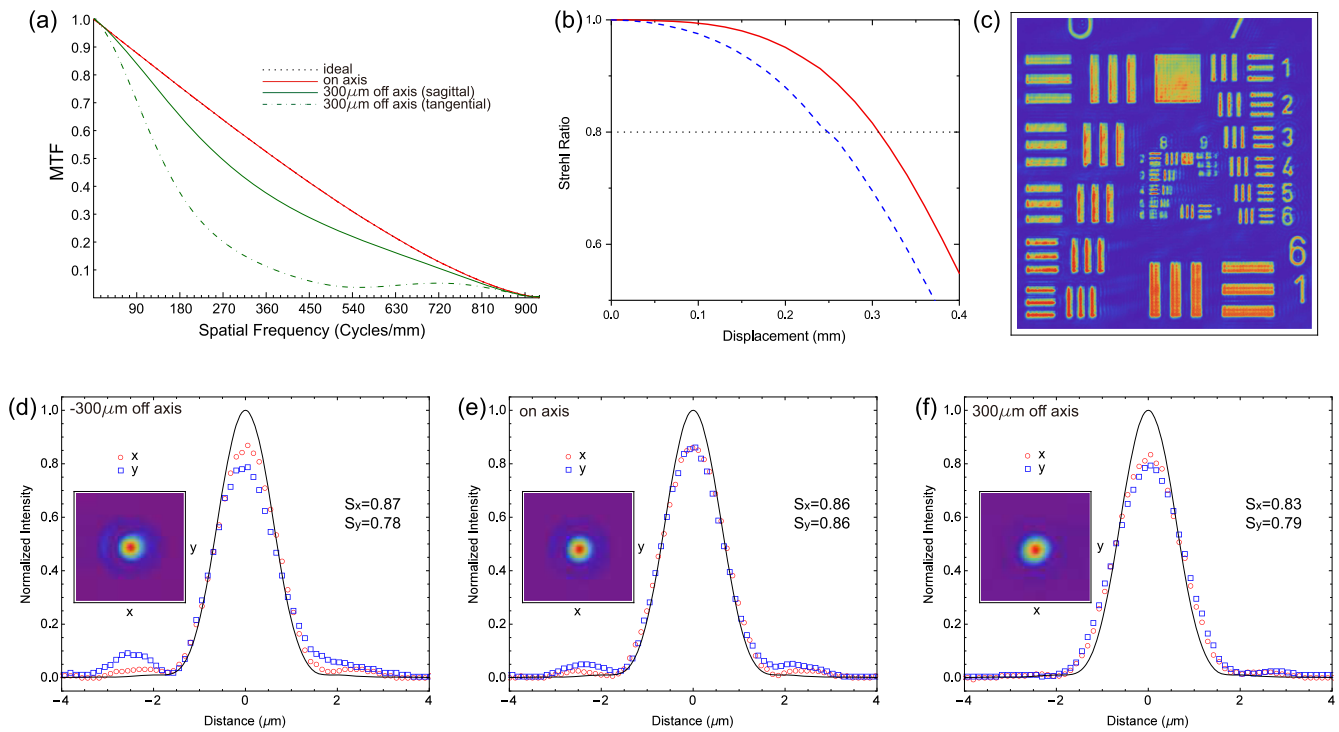


**FIG. 2.** The performance of the NA = 0.4 objective lens. (a) The simulated modulation transfer function (MTF) for focal spots on axis as well as 300  $\mu\text{m}$  off axis and the ideal diffraction limited MTF. (b) Calculated Strehl ratio. The red-solid and blue-dashed lines are the results for the original design and the design with the plano-convex lens LA4380 replaced by LA1509. The diffraction limited field of view (FOV) is defined as the displacement where the Strehl ratio  $\geq 0.8$  (the dashed line). (c) Image of the USAF 1951 resolution target. [(d)–(f)] The measured point spread function (PSF) by imaging a 1.18- $\mu\text{m}$  pinhole at the positions of  $-300 \mu\text{m}$ ,  $0 \mu\text{m}$ , and  $300 \mu\text{m}$  off the optical axis. The red circles and the blue squares are the normalized intensity distribution along the x-axis and y-axis across the intensity maxima, whereas the black curve is the convolution of a 1.18  $\mu\text{m}$  top-hat function with the point spread function. The Strehl ratios along the two axes are given by  $S_x$  and  $S_y$ . Insets of (d)–(f) are the images of the 1.18- $\mu\text{m}$  pinhole at the corresponding positions.

case, the distance between the first two lenses should be optimized to  $d = 1.6 \text{ mm}$  to get the diffraction limited condition. The corresponding performances are similar except a little smaller FOV. The calculated Strehl ratio vs off-axis displacement is also displayed

**TABLE II.** NA = 0.4 objective optimized for various wavelength with the window thickness  $d = 5 \text{ mm}$ . NA is kept as 0.4 for all the optimizations.  $\lambda$ ,  $d$ , and  $D$  are the working wavelength, distance between the first two lenses (thickness of surface 2 in Table I), and window thickness, respectively.

$\lambda$ (nm)	$d$ (mm)	EFL (mm)	FOV (mm)
405	10.5	25.0	0.18
436	9.1	25.5	0.22
486	7.2	26.3	0.29
532	5.9	26.9	0.35
589	4.7	27.4	0.42
671	3.3	28.0	0.50
780	2.0	28.6	0.57
852	1.3	28.9	0.61
1060	0.9	29.2	0.69

in Fig. 2(b) as the blue dashed line. The theoretical FOV is then 0.5 mm.

In addition to the diffraction limited performance at 852 nm and a window thickness of 5 mm, the objective can also be optimized to the diffraction limit at various working wavelengths and for various thicknesses of the flat optical window by only adjusting the distance between the first two lenses  $d$  (thickness of surface 2 in Table I). The NA is kept as 0.4 for all the optimizations. Tables II and III give the results of the optimization.

**TABLE III.** NA = 0.4 objective optimized for various window thickness  $D$  at the wavelength of 852 nm. NA is kept as 0.4 for all the optimizations.  $\lambda$ ,  $d$ , and  $D$  are the working wavelength, distance between the first two lenses (thickness of surface 2 in Table I), and window thickness, respectively.

$D$ (mm)	$d$ (mm)	EFL (mm)	FOV (mm)
7	17.3	24.2	0.6
6	7.0	27.0	0.61
5	1.3	28.9	0.61

#### IV. CONCLUSION

In summary, we present a new set of objective lens with a NA of 0.4 and a typical working distance of 18.2 mm. The diffraction-limited FOV is over 0.6 mm. The whole structure of the objective is compatible to the mostly used  $\Phi 1''$  optics and small glass cells, and thus, we believe that it is suitable for imaging and resolving single atoms for various species and vacuum cells. This objective not only provides the cold atom community an easy-obtained option to trap, resolve, and manipulate single atoms but also could be used for other applications, such as in biophysics to monitor the living cell or in industry to check the small structure over long distances.

#### ACKNOWLEDGMENTS

This work was supported by the National Natural Science Foundation of China (Grant Nos. 11634008, 11674203, 11574187, 11974223, and 11974225) and the Fund for Shanxi "1331 Project" Key Subjects Construction.

#### REFERENCES

- <sup>1</sup>T. D. Ladd, F. Jelezko, R. Laflamme, Y. Nakamura, C. Monroe, and J. L. O'Brien, *Nature* **464**, 45 (2010).
- <sup>2</sup>M. Saffman, *Nat. Sci. Rev.* **6**, 24 (2018).
- <sup>3</sup>D. S. Weiss and M. Saffman, *Phys. Today* **70**(7), 44 (2017).
- <sup>4</sup>M. Saffman, T. G. Walker, and K. Mølmer, *Rev. Mod. Phys.* **82**, 2313 (2010).
- <sup>5</sup>H. Levine, A. Keesling, G. Semeghini, A. Omran, T. T. Wang, S. Ebadi, H. Bernien, M. Greiner, V. Vuletić, H. Pichler, and M. D. Lukin, *Phys. Rev. Lett.* **123**, 170503 (2019).
- <sup>6</sup>T. M. Graham, M. Kwon, B. Grinkemeyer, Z. Marra, X. Jiang, M. T. Lichtman, Y. Sun, M. Ebert, and M. Saffman, *Phys. Rev. Lett.* **123**, 230501 (2019).
- <sup>7</sup>A. Kumar, T.-Y. Wu, F. Giraldo, and D. S. Weiss, *Nature* **561**, 83 (2018).
- <sup>8</sup>H. Labuhn, D. Barredo, S. Ravets, S. de Léséleuc, T. Macri, T. Lahaye, and A. Browaeys, *Nature* **534**, 667 (2016).
- <sup>9</sup>D. Barredo, V. Lienhard, S. de Léséleuc, T. Lahaye, and A. Browaeys, *Nature* **561**, 79 (2018).
- <sup>10</sup>M. Endres, H. Bernien, A. Keesling, H. Levine, E. R. Anschuetz, A. Krajenbrink, C. Senko, V. Vuletić, M. Greiner, and M. D. Lukin, *Science* **354**, 1024 (2016).
- <sup>11</sup>T. Xia, M. Lichtman, K. Maller, A. W. Carr, M. J. Piotrowicz, L. Isenhower, and M. Saffman, *Phys. Rev. Lett.* **114**, 100503 (2015).
- <sup>12</sup>M. Piotrowicz, M. Lichtman, K. Maller, G. Li, S. Zhang, L. Isenhower, and M. Saffman, *Phys. Rev. A* **88**, 013420 (2013).
- <sup>13</sup>K. D. Nelson, X. Li, and D. S. Weiss, *Nat. Phys.* **3**, 556 (2007).
- <sup>14</sup>W. Alt, *Optik* **113**, 142 (2002).
- <sup>15</sup>M. Weber, J. Volz, K. Saucke, C. Kurtsiefer, and H. Weinfurter, *Phys. Rev. A* **73**, 043406 (2006).
- <sup>16</sup>N. Piro, F. Rohde, C. Schuck, M. Almendros, J. Huwer, J. Ghosh, A. Haase, M. Hennrich, F. Dubin, and J. Eschner, *Nat. Phys.* **7**, 17 (2011).
- <sup>17</sup>B. Zimmermann, T. Müller, J. Meineke, T. Esslinger, and H. Moritz, *New J. Phys.* **13**, 043007 (2011).
- <sup>18</sup>X. Li, F. Zhou, M. Ke, P. Xu, X.-D. He, J. Wang, and M.-S. Zhan, *Appl. Opt.* **57**, 7584 (2018).
- <sup>19</sup>J. D. Pritchard, J. A. Isaacs, and M. Saffman, *Rev. Sci. Instrum.* **87**, 073107 (2016).
- <sup>20</sup>L. M. Bennie, P. T. Starkey, M. Jasperse, C. J. Billington, R. P. Anderson, and L. D. Turner, *Opt. Express* **21**, 9011 (2013).
- <sup>21</sup>H. Gross, H. Zügge, M. Peschka, and F. Blechinger, *Handbook of Optical Systems, Aberration Theory and Correction of Optical Systems* (Wiley-VCH, 2015), pp. 1–756.